Optimal analysis on the performance of an irreversible harmonic quantum Brayton refrigeration cycle

Bihong Lin
Department of Physics, Xiamen University, Xiamen 361005, People's Republic of China
and Department of Physics, Quanzhou Normal College, Quanzhou 362000, People's Republic of China

Jincan Chen*
CCAST (World Laboratory), P.O. 8730, Beijing 100080, People's Republic of China
and Department of Physics, Xiamen University, Xiamen 361005, People's Republic of China†
(Received 28 May 2003; published 21 November 2003)

An irreversible model of a quantum refrigeration cycle working with many noninteracting harmonic oscillators is established. The refrigeration cycle consists of two adiabatic and two constant-frequency processes. The general performance characteristics of the cycle are investigated, based on the quantum master equation and the semigroup approach. The expressions for several important performance parameters such as the coefficient of performance, cooling rate, power input, and rate of entropy production are derived. By using numerical solutions, the cooling rate of the refrigeration cycle subject to finite cycle duration is optimized. The maximum cooling rate and the corresponding parameters are calculated numerically. The optimal region of the coefficient of performance and the optimal ranges of temperatures of the working substance and times spent on the two constant-frequency processes are determined. Moreover, the optimal performance of the cycle in the high-temperature limit is compared with that of a classical Brayton refrigerator working with an ideal gas. The results obtained here show that in the high-temperature limit a harmonic quantum Brayton cycle may be equivalent to a classical Brayton cycle.

DOI: 10.1103/PhysRevE.68.056117 PACS number(s): 05.70.−a, 07.20.Mc, 44.90.+c

I. INTRODUCTION

The harmonic oscillator and spin systems are two typical mechanical systems in quantum physics and have been widely applied to all kinds of practicaly physical problems since the beginning of quantum theory. Recently, several authors have intensively investigated the performance characteristics of quantum thermodynamic cycles working with harmonic oscillator systems [1–6] or spin systems [7–12], based on the quantum master equation and the semigroup approach. Many meaningful conclusions have been obtained. Quantum thermodynamic cycles have become an interesting research subject. Investigation of the performance of quantum thermodynamic cycles has been a major source of thermodynamic insight and led to a connection between abstract theory and realizable physical phenomena. Quantum models of thermodynamic cycles show a remarkable similarity to classical thermodynamic cycles obeying macroscopic dynamics. The investigation of them will be helpful to deeply understand the relationship and distinguish between the quantum and classical thermodynamic cycles.

Like classical thermodynamic cycles, quantum thermodynamic cycles using harmonic oscillator or spin systems as the working substance may have different typical cycle models. For example, when harmonic oscillator systems are used as the working substance, we have the quantum Carnot cycle [2,3,5,6] consisting of two isothermal and two adiabatic (i.e., constant-population) processes, the Ericsson cycle consisting of two isothermal and two constant-frequency processes [1,4], the Brayton cycle consisting of two adiabatic (i.e., constant-population) and two constant-frequency processes, etc. The quantum Carnot cycle, Ericsson cycle, and Brayton cycle are obviously three models of the most important quantum thermodynamic cycles working with harmonic oscillator systems. The optimal performance of the quantum Carnot cycle and Ericsson cycle has been investigated and many significant results have been obtained [1–6]. However, so far the optimal performance of the quantum Brayton refrigeration cycle working with harmonic oscillator systems has rarely been studied. Thus, it is of great significance to study the optimal performance of this class of quantum thermodynamic cycles. It is also worthwhile to point out that a similar cycle model, which consists of two adiabatic (i.e., constant-polarization) and two isomagnetic field processes, has been used to analyze the performance of an irreversible quantum refrigeration cycle working with many noninteracting spin-1/2 systems, and many significant results have been obtained [9]. Because the cycle working substance adopted here is different from that used in Ref. [9], it may be expected that some results different from those derived in Ref. [9] will be obtained.

In this paper, the optimal performance of a quantum refrigeration cycle working with many noninteracting harmonic oscillators and consisting of two adiabatic and two constant-frequency processes is investigated, based on the dynamical semigroup approach of the quantum theory of open systems. The general expressions for several important parameters, such as the coefficient of performance, cooling

*Author to whom correspondence should be addressed. Electronic address: jcchen@xmu.edu.cn
†Mailing address.

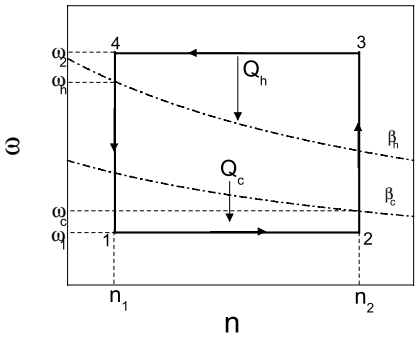

FIG. 1. The ω-n diagram of an irreversible harmonic quantum refrigeration cycle, where ω is in joules.

rate, power input, and rate of entropy production, are derived. The important performance parameters are optimized and the general performance characteristics of the cycle are analyzed. The optimaly operating regions of some important performance parameters of the cycle are determined.

II. A QUANTUM CYCLE MODEL

Figure 1 shows schematically the ω-n diagram of an irreversible quantum refrigeration cycle operating between two heat reservoirs at temperatures T_h and T_c. The refrigeration cycle consists of two adiabatic and two constant-frequency processes. The working substance of the cycle is composed of many noninteracting harmonic oscillators. For convenience, throughout this paper ''temperature'' will refer to β rather than T. In the cycle, two adiabatic processes are connected by two constant-frequency processes $\omega=\omega_1$ and $\omega=\omega_2$ with $\omega_2>\omega_1$. The two constant-frequency processes in the harmonic quantum refrigeration cycle correspond to the two constant-pressure processes in a gas Brayton refrigeration cycle, while the two adiabatic processes in the cycle are identical to two processes where the populations of the harmonic oscillators $n=n_1$ and n_2 are kept constant [3]. Thus, the quantum refrigeration cycle shown in Fig. 1 may be referred to as the harmonic quantum Brayton refrigeration cycle.

In the two constant-frequency processes, the oscillators are, respectively, coupled to the heat reservoirs at constant temperatures $\beta=\beta_h$ and $\beta=\beta_c$, and the amounts of heat exchange between the working substance and the heat reservoirs are represented by Q_h and Q_c. Due to the finite rate of heat transfer between the working substance and the heat reservoirs, the temperatures β_1, β_2, β_3, and β_4 of the working substance in states 1, 2, 3, and 4 are different from those of the heat reservoirs and there is a relation $\beta_1>\beta_2 \geqslant \beta_c>\beta_h \geqslant \beta_4>\beta_3$. For a harmonic oscillator system, Bose-Einstein condensation (BEC) must be considered. Consequently, the lowest temperature β_1 of the working substance must be restricted to being higher than the critical temperature of BEC of the harmonic oscillators.

III. THE COEFFICIENT OF PERFORMANCE AND WORK INPUT

Based on statistical mechanics, the population of the oscillators n can be obtained from the Bose-Einstein distribution [13], i.e.,

$$n=\frac{1}{\exp(\beta'\omega)-1}, \tag{1}$$

where $\omega>0$ is the frequency of the oscillator, $\beta'=1/T$, and T is the absolute temperature in energy units. Using Eq. (1) and Fig. 1, one can obtain the following relations:

$$\beta_1\omega_1=\beta_4\omega_2 \tag{2}$$

and

$$\beta_2\omega_1=\beta_3\omega_2. \tag{3}$$

It is thus clear that for a harmonic quantum Brayton refrigeration cycle there is an important relation $\beta_1/\beta_2=\beta_4/\beta_3$, which restricts the temperatures of the four states 1, 2, 3, and 4 in Fig. 1. It is of interest to note that this important relation is identical with that of a Brayton refrigeration cycle working with an ideal gas.

For a harmonic oscillator system, the Hamiltonian is described in the following form [3,14]:

$$\hat{\mathbf{H}}(t)=\omega(t)\hat{\mathbf{N}}=\omega(t)\hat{\mathbf{a}}^{\dagger}\hat{\mathbf{a}}, \tag{4}$$

where $\hat{\mathbf{a}}^{\dagger}$ and $\hat{\mathbf{a}}$ are the bosonic creation and annihilation operators and $\hat{\mathbf{N}}=\hat{\mathbf{a}}^{\dagger}\hat{\mathbf{a}}$ is the number operator. The internal energy of the harmonic oscillator system is of the expectation value of the Hamiltonian, i.e.,

$$E=\langle\hat{\mathbf{H}}\rangle=\omega(t)\langle\hat{\mathbf{N}}\rangle=\omega(t)n, \tag{5}$$

where $\langle\hat{\mathbf{N}}\rangle=n$. For a harmonic quantum refrigerator, the internal energy of the working substance may be changed by changing either the frequency or the population of the oscillators. The cycle operation is followed by changes in the observables of the working substance. Based on the semigroup formalism [3,15], the equation of motion of an operator $\hat{\mathbf{X}}$ in the Heisenberg picture is given by the quantum master equation [3,12,15–17] (throughout this paper we adopt $\hbar=1$ for simplicity), i.e.,

$$\frac{d\hat{\mathbf{X}}}{dt}=i[\hat{\mathbf{H}},\hat{\mathbf{X}}]+\frac{\partial\hat{\mathbf{X}}}{\partial t}+L_D(\hat{\mathbf{X}}), \tag{6}$$

where $L_D(\hat{\mathbf{X}})=\Sigma_\alpha\gamma_\alpha(\hat{\mathbf{V}}_\alpha^{\dagger}[\hat{\mathbf{X}},\hat{\mathbf{V}}_\alpha]+[\hat{\mathbf{V}}_\alpha^{\dagger},\hat{\mathbf{X}}]\hat{\mathbf{V}}_\alpha)$ is a dissipation term and originates from the thermal coupling between the working substance and the heat reservoir, γ_α are phenomenological positive coefficients, and $\hat{\mathbf{V}}_\alpha^{\dagger}$ and $\hat{\mathbf{V}}_\alpha$ are operators in the Hilbert space of the system and are Hermitian conjugates. For a harmonic oscillator system, $\hat{\mathbf{V}}_\alpha^{\dagger}$ and $\hat{\mathbf{V}}_\alpha$ may be chosen to be the bosonic annihilation and creation operators $\hat{\mathbf{a}}^{\dagger}$ and $\hat{\mathbf{a}}$. Substituting $\hat{\mathbf{X}}$ in Eq. (6) by $\hat{H}$ and using Eq. (5), one obtains the rate of change of the internal energy as

$$\frac{dE}{dt}=\frac{d}{dt}\langle\hat{\mathbf{H}}\rangle=\left\langle\frac{\partial\hat{\mathbf{H}}}{\partial t}\right\rangle+\langle L_D(\hat{\mathbf{H}})\rangle$$
$$=\langle\hat{\mathbf{N}}\rangle\frac{d\omega}{dt}+\omega\langle L_D(\hat{\mathbf{N}})\rangle=n\frac{d\omega}{dt}+\omega\frac{dn}{dt}. \quad (7)$$

It is thus clear that Eq. (7) is the time derivative of the first law of thermodynamics [3,16–19] for a harmonic oscillator system. Comparing Eq. (7) with the differential form of the first law of thermodynamics, $dE/dt=dW/dt+dQ/dt$, one can identify the instantaneous power and heat flow [3,18,19] as

$$P=\frac{dW}{dt}=\left\langle\frac{\partial\hat{\mathbf{H}}}{\partial t}\right\rangle=n\frac{d\omega}{dt} \quad (8)$$

and

$$\frac{dQ}{dt}=\langle L_D(\hat{\mathbf{H}})\rangle=\omega\frac{dn}{dt}. \quad (9)$$

Using Eqs. (1) and (9), one can find that the amounts of heat exchange in the two constant-frequency processes of the cycle are given, respectively, by

$$Q_c=Q_{12}=\int_1^2 dQ=\int_{n_1}^{n_2}\omega_1 dn=\omega_1(n_2-n_1)$$
$$=\frac{\omega_1(e^{\beta_4\omega_2}-e^{\beta_2\omega_1})}{(e^{\beta_4\omega_2}-1)(e^{\beta_2\omega_1}-1)} \quad (10)$$

and

$$Q_h=Q_{34}=\int_3^4 dQ=\int_{n_2}^{n_1}\omega_2 dn$$
$$=\omega_2(n_1-n_2)=\frac{\omega_2(e^{\beta_2\omega_1}-e^{\beta_4\omega_2})}{(e^{\beta_4\omega_2}-1)(e^{\beta_2\omega_1}-1)}. \quad (11)$$

When a cycle is finished and the working substance returns to the original state, the change of internal energy is equal to zero, i.e., $\oint dE=0$. The work input per cycle is $W=\oint n d\omega=-\oint dQ=-\oint\omega dn$. Using Eqs. (10) and (11), one can obtain the work input per cycle as

$$W=|Q_h+Q_c|=(\omega_2-\omega_1)(n_2-n_1)$$
$$=\frac{(\omega_2-\omega_1)(e^{\beta_4\omega_2}-e^{\beta_2\omega_1})}{(e^{\beta_4\omega_2}-1)(e^{\beta_2\omega_1}-1)}. \quad (12)$$

From Eqs. (10) and (12), we can derive the coefficient of performance of a quantum Brayton refrigeration cycle working with harmonic oscillators as

$$\varepsilon=\frac{Q_c}{W}=\frac{\omega_1}{\omega_2-\omega_1}. \quad (13)$$

IV. CYCLE PERIOD

In order to analyze further the optimal performance of the harmonic quantum Brayton refrigeration cycle, the period of the cycle has to be calculated. For this end, we begin to solve the equation of motion that determines the time evolution of the populations of the harmonic oscillators. Substituting $\hat{\mathbf{a}}^\dagger$, $\hat{\mathbf{a}}$, $\hat{\mathbf{H}}$, and $\hat{\mathbf{X}}=\hat{\mathbf{N}}$ into Eq. (6), one can prove [3] that

$$\frac{dn}{dt}=-2ae^{q\beta\omega}[(e^{\beta\omega}-1)n-1], \quad (14)$$

where $a>0$, $-1<q<0$, and β, ω, and n are, in general, dependent on time [3]. The explicit quantum mechanical nature of a refrigerator working with harmonic oscillators is manifested by the dual character of ω, i.e., $\hbar\omega$ ($\hbar=1$) defines the energy level structure of the refrigeration cycle and ω is the frequency of the oscillators so that ω^{-1} defines an intrinsic time scale. This implicitly assumes an instantaneous response of the heat reservoir to changes in the frequency ω, and the time duration of a process should be long enough so that resonance conditions are established instantaneously. This means that the time duration for each process has to be much larger than the intrinsic time scale [3]. Thus, the change of ω with time is small. This point can also be directly obtained from Eq. (1).

Using Eq. (14), one can obtain the expression for the time evolution as

$$t=-\frac{1}{2a}\int_{n_i}^{n_f}\frac{dn}{e^{q\beta\omega}[(e^{\beta\omega}-1)n-1]}, \quad (15)$$

where n_i and n_f are the initial and final values of n along a given path $n(\beta',\omega)$. Equation (15) is a general expression of the time evolution for a harmonic oscillator system coupled with a heat bath.

According to Eq. (15), one can calculate the time of the heat-exchange process between the working substance and the heat reservoir. Substituting $n(\beta')=1/(e^{\beta'\omega_1}-1)$, $\beta=\beta_c$, $n_i=n_i(\beta_1,\omega_1)$, and $n_f=n_f(\beta_2,\omega_1)$ into Eq. (15) and using Eqs. (2) and (3), we can obtain the time spent on the constant-frequency process with $\omega=\omega_1$ as

$$t_1=\frac{1}{2ae^{q\beta_c\omega_1}}\int_{\beta_1}^{\beta_2}\frac{d(e^{\beta'\omega_1})}{(e^{\beta'\omega_1}-1)(e^{\beta_c\omega_1}-e^{\beta'\omega_1})}=C_1\ln A, \quad (16)$$

where $A=(e^{\beta_2\omega_1}-1)(e^{\beta_c\omega_1}-e^{\beta_4\omega_2})/(e^{\beta_4\omega_2}-1)(e^{\beta_c\omega_1}-e^{\beta_2\omega_1})$ and $C_1=1/[2ae^{q\beta_c\omega_1}(e^{\beta_c\omega_1}-1)]$. Similarly, substituting $n(\beta')=1/(e^{\beta'\omega_2}-1)$, $\beta=\beta_h$, $n_i=n_i(\beta_3,\omega_2)$, and $n_f=n_f(\beta_4,\omega_2)$ into Eq. (15) and using Eqs. (2) and (3), we can obtain the time spent on the constant-frequency process with $\omega=\omega_2$ as

$$t_2=\frac{1}{2ae^{q\beta_h\omega_2}}\int_{\beta_3}^{\beta_4}\frac{d(e^{\beta'\omega_2})}{(e^{\beta'\omega_2}-1)(e^{\beta_h\omega_2}-e^{\beta'\omega_2})}=C_2\ln B, \quad (17)$$

where $B=(e^{\beta_4\omega_2}-1)(e^{\beta_h\omega_2}-e^{\beta_2\omega_1})/(e^{\beta_2\omega_1}-1)(e^{\beta_h\omega_2}-e^{\beta_4\omega_2})$ and $C_2=1/[2ae^{q\beta_h\omega_2}(e^{\beta_h\omega_2}-1)]$. It can be seen from Eq. (9) that in two adiabatic processes the amounts of heat exchange between the working substance and the surroundings are equal to zero and the times spent on the two adiabatic processes are negligible [12] compared with the constant-frequency processes. Consequently, the cycle period is given by

$$\tau=t_1+t_2=C_1\ln A+C_2\ln B. \tag{18}$$

V. OPTIMIZATION ON PERFORMANCE PARAMETERS

In addition to the coefficient of performance, the cooling rate, power input, and rate of entropy production are also three of the important parameters often considered in the optimal design and theoretical analysis of refrigerators. Using Eqs. (10)–(12) and (18), we can find that the expressions for the cooling rate R, power input P, and rate of entropy production σ are, respectively, given by

$$R=\frac{Q_c}{\tau}=\frac{\omega_1(e^{\beta_4\omega_2}-e^{\beta_2\omega_1})}{(e^{\beta_2\omega_1}-1)(e^{\beta_4\omega_2}-1)(C_1\ln A+C_2\ln B)}, \tag{19}$$

$$P=\frac{W}{\tau}=\frac{(\omega_2-\omega_1)(e^{\beta_4\omega_2}-e^{\beta_2\omega_1})}{(e^{\beta_2\omega_1}-1)(e^{\beta_4\omega_2}-1)(C_1\ln A+C_2\ln B)}, \tag{20}$$

and

$$\sigma=\frac{\Delta S}{\tau}=\frac{(\beta_h\omega_2-\beta_c\omega_1)(e^{\beta_4\omega_2}-e^{\beta_2\omega_1})}{(e^{\beta_2\omega_1}-1)(e^{\beta_4\omega_2}-1)(C_1\ln A+C_2\ln B)}. \tag{21}$$

With the help of the above equations, one can optimize these important performance parameters of the harmonic quantum Brayton refrigeration cycle.

It is clearly seen from Eqs. (13) and (19) that the cooling rate is zero when $\varepsilon=0$ or $\varepsilon=\varepsilon_r$, where $\varepsilon_r=\omega_c/(\omega_h-\omega_c)$ is the maximum coefficient of performance of a harmonic quantum Brayton refrigeration cycle and the frequencies ω_c and ω_h are, respectively, the upper and lower bounds of the frequencies ω_1 and ω_2 of the oscillators. This implies that, when the coefficient of performance is equal to some value, the cooling rate has a maximum. Using Eq. (19) and the extremal condition $\partial R/\partial\omega_1=0$, we can obtain the following equation:

$$\frac{\tau}{C_1\beta_c}-\omega_1\left\{\frac{(n_2-n_1)e^{\beta_c\omega_1}}{[n_1(e^{\beta_c\omega_1}-1)-1][n_2(e^{\beta_c\omega_1}-1)-1]}-\frac{(q+1)e^{\beta_c\omega_1}-q}{(e^{\beta_c\omega_1}-1)}\ln A\right\}=0. \tag{22}$$

Equation (22) gives the optimal relation between $\beta_2(\omega_1)$ and $\beta_4(\omega_2)$ for given q, β_h, β_c, ω_h, and ω_c, but it is too complicated to yield a simple analytical solution. However, for given q, β_h, β_c, ω_h, and ω_c, the $R^*-\varepsilon$, $P^*-\varepsilon$, R^*-P^*, $\sigma^*-\varepsilon$, and $\beta_i/\beta_j-\varepsilon$ characteristic curves can be plotted by using Eqs. (13) and (19)–(22), as shown in Figs. 2–6, where $R^*=R/(2a\omega_c)$, $P^*=P/(2a\omega_c)$, and $\sigma^*=kT_h\sigma/(2a\omega_c)$ are, respectively, the dimensionless cooling rate, power input, and rate of entropy production. In these figures, the parameters $kT_h=2.0J$, $kT_c=1.0J$, $\omega_h=2.05J$, $\omega_c=1.0J$, and $q=-0.5$ are adopted [19].

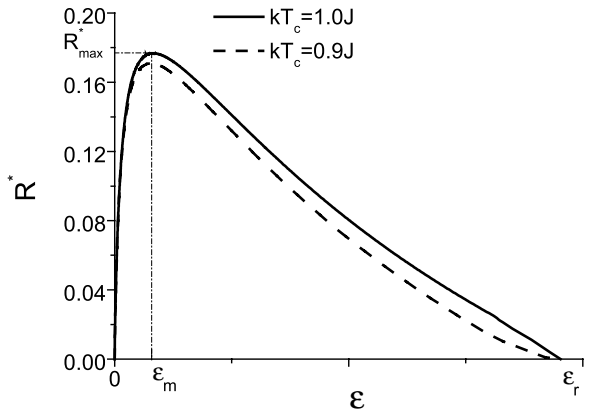

FIG. 2. The dimensionless cooling rate $R^*=R/(2a\omega_c)$ versus the coefficient of performance ε for the parameters $kT_h=2.0J$, $\omega_h=2.05J$, $\omega_c=1.0J$, and $q=-0.5$. Dashed and solid curves correspond to the cases of $kT_c=0.9J$ and $kT_c=1.0J$, respectively.

It is seen from the curves in Fig. 2 that there exists a maximum cooling rate $R_{\max}$ and a corresponding coefficient of performance ε_m for a set of given parameters q, β_h, β_c, ω_h, and ω_c. Obviously, for different given parameters, the maximum cooling rate $R_{\max}$ and corresponding coefficient of performance ε_m will be different. For example, for given ω_c/ω_h, the larger is the temperature ratio T_c/T_h of the two heat reservoirs, the larger are the maximum cooling rate and corresponding coefficient of performance; for given T_c/T_h, the lower is the frequency ratio ω_c/ω_h of the oscillators, the larger is the maximum cooling rate while the lower is the corresponding coefficient of performance, as indicated in Table I.

On the other hand, it is also seen from the curves in Fig. 2 that when $R<R_{\max}$ there are two different coefficients of

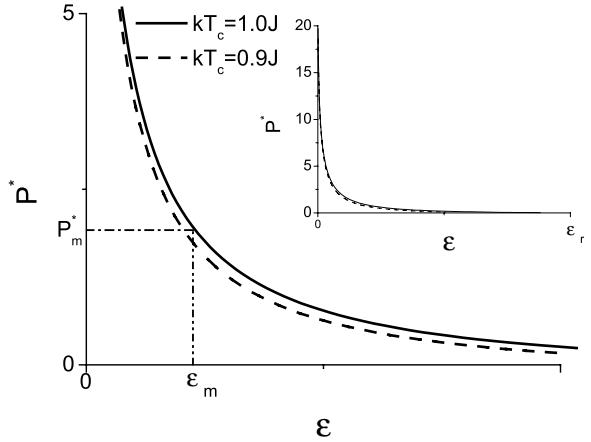

FIG. 3. The dimensionless power input $P^*=P/(2a\omega_c)$ versus the coefficient of performance ε. The values of the relevant parameters are the same as those used in Fig. 2.

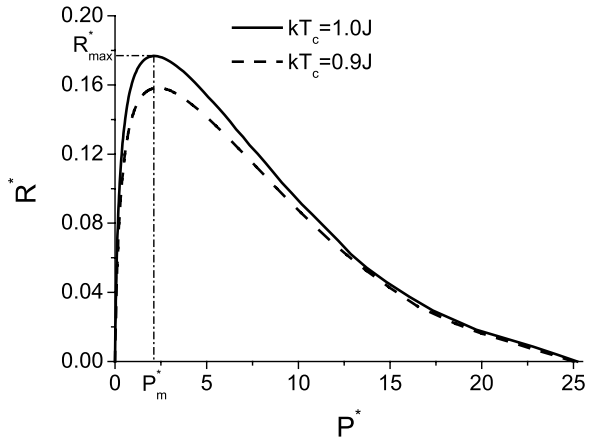

FIG. 4. The dimensionless cooling rate R^* versus the dimensionless power input P^*. The values of the relevant parameters are the same as those used in Fig. 2.

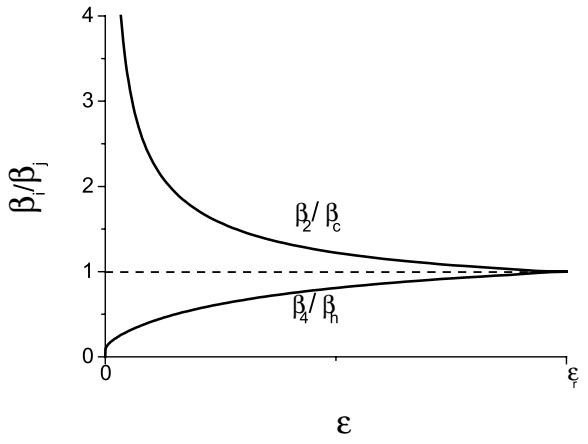

FIG. 6. The β_4/β_h-ε and β_2/β_c-ε characteristic curves. The values of the relevant parameters are the same as those used in Fig. 2.

performance for a given cooling rate R, where one is larger than ε_m and the other is smaller than ε_m. When $\varepsilon<\varepsilon_m$, the cooling rate decreases as the coefficient of performance decreases. It is thus clear that the region of $\varepsilon<\varepsilon_m$ is not optimal for a harmonic quantum Brayton refrigeration cycle. Consequently, the optimal region of the coefficient of performance should be

$$\varepsilon_m \leqslant \varepsilon < \varepsilon_r . \tag{23}$$

When a quantum Brayton refrigeration cycle is operated in this region, the cooling rate will increase as the coefficient of performance decreases, and vice versa. This indicates that ε_m is an important parameter for the harmonic quantum Brayton refrigeration cycle. It determines the allowable value of the lower bound of the optimal coefficient of performance.

Analyzing Eq. (23) and Figs. 2–6, we can find further that the optimal values of the power input should be

$$P \leqslant P_m , \tag{24}$$

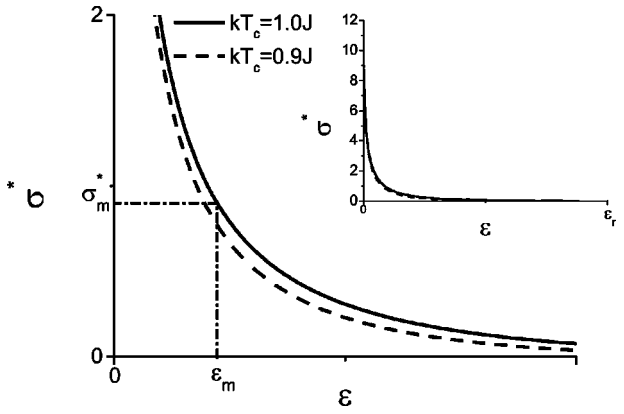

FIG. 5. The dimensionless rate of entropy production $\sigma^* = kT_h\sigma/(2a\omega_c)$ versus the coefficient of performance ε. The values of the relevant parameters are the same as those used in Fig. 2.

and that the optimal ranges of the ''temperatures'' of the working substance in states 2 and 4 in the two constant-frequency processes should be

$$\beta_{2m} \geqslant \beta_2 > \beta_c \tag{25}$$

and

$$\beta_{4m} \leqslant \beta_4 < \beta_h , \tag{26}$$

where the values of P_m, β_{2m}, and β_{4m} can be calculated from Eqs. (19), (20), and (22) and have been listed in Table I. Using Eqs. (2), (3), (25), and (26), we can obtain the optimal ranges of the lowest and highest ''temperatures'' β_1 and β_3 of the working substance in the two constant-frequency processes, respectively, as

$$\beta_{1m} = \beta_{4m}\omega_2/\omega_1 \leqslant \beta_1 < \beta_h\omega_2/\omega_1 \tag{27}$$

and

$$\beta_{3m} = \beta_{2m}\omega_1/\omega_2 \geqslant \beta_3 > \beta_c\omega_1/\omega_2 . \tag{28}$$

The above results clearly show that P_m, β_{1m}, β_{2m}, β_{3m}, and β_{4m} are also several important performance parameters for a harmonic quantum Brayton refrigeration cycle and Eqs. (24)–(28) provide several significant criteria for the selection of optimaly operating conditions. In addition, using Eqs. (16), (17), (22), and (23), one can find that the times t_1 and

TABLE I. Optimal parameters at the maximum cooling rate for given T_c/T_h, ω_c/ω_h, and $q=-0.5$.

T_c/T_h	ω_c/ω_h	T_{2m}/T_{4m}	$R_{\max}$	ε_m	P_m	σ_m
0.48	0.4	0.08	0.1948	0.0754	2.5826	1.1278
	0.49	0.07	0.1709	0.0779	2.1943	0.9554
0.50	0.4	0.09	0.2001	0.0777	2.5825	1.1909
	0.49	0.08	0.1767	0.0850	2.0883	0.9558
0.52	0.4	0.10	0.2070	0.0800	2.5818	1.2639
	0.48	0.09	0.1828	0.0878	2.0824	1.0094

t_2 spent on the two constant-frequency processes of the cycle should be controlled to satisfy the following conditions:

$$t_1 \geqslant t_{1m} \tag{29}$$

and

$$t_2 \geqslant t_{2m}, \tag{30}$$

where

$$t_{1m}=\frac{1}{2a e^{q\beta_c\omega_1}(e^{\beta_c\omega_1}-1)}\ln\left[\frac{(e^{\beta_{2m}\omega_1}-1)(e^{\beta_c\omega_1}-e^{\beta_{4m}\omega_2})}{(e^{\beta_{4m}\omega_2}-1)(e^{\beta_c\omega_1}-e^{\beta_{2m}\omega_1})}\right]$$

and

$$t_{2m}=\frac{1}{2a e^{q\beta_h\omega_2}(e^{\beta_h\omega_2}-1)}\ln\left[\frac{(e^{\beta_{4m}\omega_2}-1)(e^{\beta_h\omega_2}-e^{\beta_{2m}\omega_1})}{(e^{\beta_{2m}\omega_1}-1)(e^{\beta_h\omega_2}-e^{\beta_{4m}\omega_2})}\right].$$

If not, the quantum refrigeration cycle would not be operating in the rational region.

Figures 3–6 show that the power input P, rate of entropy production σ, and temperature ratio β_2/β_c are monotonically decreasing functions of the coefficient of performance ε, while the other temperature ratio β_4/β_h is a monotonically increasing function of the coefficient of performance ε. The cooling rate R is not a monotonic function of the power input P. When $\beta_2=\beta_c$ and $\beta_4=\beta_h$, $\varepsilon=\varepsilon_r$, $R=0$, $P=0$, and $\sigma=0$. In such a case, the refrigerator attains its maximum coefficient of performance, but its cooling rate is equal to zero so that it loses its refrigeration role.

VI. PERFORMANCE CHARACTERISTICS AT HIGH TEMPERATURES

When the temperatures of the two heat reservoirs are high enough, i.e., $\beta\omega \ll 1$, the results obtained above can be simplified. For example, Eqs. (16), (17), and (19)–(22) can be simplified, respectively, as

$$t_1=\frac{1}{2a\beta_c\omega_1}\ln\left[\frac{\beta_2(\beta_4\omega_2-\beta_c\omega_1)}{\beta_4\omega_2(\beta_2-\beta_c)}\right]=\frac{1}{2a\beta_c\omega_1}\ln\left[\frac{\beta_2(\beta_1-\beta_c)}{\beta_1(\beta_2-\beta_c)}\right], \tag{31}$$

$$t_2=\frac{1}{2a\beta_h\omega_2}\ln\left[\frac{\beta_4(\beta_h\omega_2-\beta_2\omega_1)}{\beta_2\omega_1(\beta_h-\beta_4)}\right]=\frac{1}{2a\beta_h\omega_2}\ln\left[\frac{\beta_4(\beta_h-\beta_3)}{\beta_3(\beta_h-\beta_4)}\right], \tag{32}$$

$$R=\frac{\beta_4\omega_2-\beta_2\omega_1}{\beta_2\beta_4\omega_2(t_1+t_2)}, \tag{33}$$

$$P=\frac{(\omega_2-\omega_1)(\beta_4\omega_2-\beta_2\omega_1)}{\beta_2\beta_4\omega_1\omega_2(t_1+t_2)}, \tag{34}$$

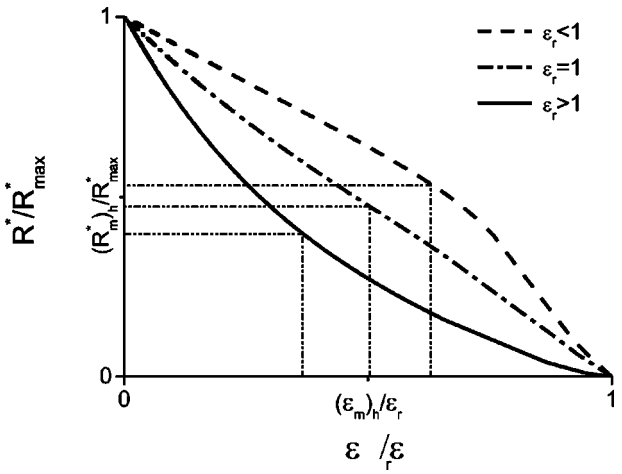

FIG. 7. The dimensionless cooling rate R^* versus the coefficient of performance ε in the high-temperature limit. Dashed ($\omega_c=2.0J$), dash-dotted ($\omega_c=3.0J$), and solid ($\omega_c=4.0J$) curves are presented for the parameters $kT_h=500J$, $kT_c=400J$, $\omega_h=6.0J$, and $q=-0.5$. The parameters $(R_m)_h$ and $(\varepsilon_m)_h$ represent the cooling rate and coefficient of performance at the maximum ($R\varepsilon$), respectively.

$$\sigma=\frac{(\beta_4\omega_2-\beta_2\omega_1)(\beta_h\omega_2-\beta_c\omega_1)}{\beta_2\beta_4\omega_1\omega_2(t_1+t_2)}, \tag{35}$$

and

$$2a\beta_c\tau-\frac{\beta_c\beta_2 n_2(n_2-n_1)}{(\beta_2-\beta_c)(n_2\beta_2-n_1\beta_c)}+n_2\beta_2\ln\left(\frac{n_2\beta_2-n_1\beta_c}{n_2\beta_2-n_2\beta_c}\right)=0. \tag{36}$$

Using Eqs. (13), (31)–(33), and (36), we can generate the R^*-ε characteristic curves for given β_h, β_c, ω_h, and ω_c, as shown in Fig. 7, where the parameters $kT_h=500J$, $kT_c=400J$, $\omega_c=2.0J$ (dashed curve), $3.0J$ (dash-dotted curve), $4.0J$ (solid curve), and $\omega_h=6.0J$ are adopted. It is clearly seen from the curves in Fig. 7 that at high temperatures the R^*-ε curves of an irreversible harmonic quantum Brayton refrigeration cycle are different from those of the refrigeration cycle at low temperatures. The cooling rate R decreases monotonically as the coefficient of performance ε increases. When $\varepsilon_r \approx 1$, the R^*-ε curve is approximately a straight line, i.e., the cooling rate is approximately a linearly decreasing function of the coefficient of performance. When the condition $\varepsilon_r \approx 1$ is not satisfied, the R^*-ε curve is convex for $\varepsilon_r > 1$, while the R^*-ε curve is concave for $\varepsilon_r < 1$. When $\varepsilon=0$, the cooling rate attains its maximum value $R_{\max}$. Using Eqs. (33) and (36), one can obtain the maximum cooling rate as

$$R_{\max}=\frac{(n_2-n_1)\omega_{1m}}{T_c/(2a\omega_{1m})\ln[(T_c-n_1\omega_{1m})/(T_c-n_2\omega_{1m})]}, \tag{37}$$

where $\omega_{1m}=2(T_c-n_2\omega_{1m})(T_c-n_1\omega_{1m})\ln[(T_c-n_1\omega_{1m})/(T_c-n_2\omega_{1m})]/[T_c(n_2-n_1)]$. In this case, an infinite power input is

required. This shows that the cooling rate of a practical refrigerator cannot approach $R_{\max}$. Thus, the states of $R=R_{\max}$ and $\varepsilon=\varepsilon_r$ are two limit states and the refrigeration cycle cannot be operated in these two states, so that consideration must be given to both the coefficient of performance and the cooling rate. Equations (13), (31)–(33), and (36) just provide some theoretical bases for the question of how to choose the two parameters reasonably. For example, when we pay equal attention to both the coefficient of performance ε and the cooling rate R, the multiplication εR may be taken as an objective function [20]. The cooling rate $(R_m)_h$ and coefficient of performance $(\varepsilon_m)_h$ at the maximum εR condition can be calculated, as shown in Fig. 7. It is clearly seen directly from the curves in Fig. 7 that there is a relation $(\varepsilon_m)_h/\varepsilon_r \approx (R_m)_h/R_{\max} \approx 1/2$ for $\varepsilon_r=1$.

On the other hand, using Eqs. (2), (3), (31), (32), and (1), Eqs. (13), (33), and (34) at high temperatures can be written as

$$\varepsilon=\frac{T_2-T_1}{(T_3-T_4)-(T_2-T_1)}, \tag{38}$$

$$R=\frac{T_2-T_1}{T_c/(2a\omega_1)\ln[(T_c-T_1)/(T_c-T_2)]+T_h/(2a\omega_2)\ln[(T_3-T_h)/(T_4-T_h)]}, \tag{39}$$

and

$$P=\frac{(T_3-T_4)-(T_2-T_1)}{T_c/(2a\omega_1)\ln[(T_c-T_1)/(T_c-T_2)]+T_h/(2a\omega_2)\ln[(T_3-T_h)/(T_4-T_h)]}. \tag{40}$$

It is of interest to compare the expressions for the coefficient of performance, cooling rate, and power input obtained here with those derived from a classical Brayton refrigeration cycle using an ideal gas as the working substance. When the influence of finite-rate heat transfer between the working substance and the heat reservoirs on the performance of a classical Brayton refrigeration cycle is considered and the heat transfer is assumed to obey a Newtonian law, the coefficient of performance, cooling rate, and power input of the classical Brayton refrigeration cycle are given by

$$\varepsilon=\frac{Q_c}{W}=\frac{T_2-T_1}{(T_3-T_4)-(T_2-T_1)}, \tag{41}$$

$$R=\frac{Q_c}{\tau}=\frac{T_2-T_1}{(T_2-T_1)/[U_C A_C(\mathcal{D}_C)]+(T_3-T_4)/[U_H A_H(\mathcal{D}_H)]}, \tag{42}$$

$$P=\frac{W}{\tau}=\frac{(T_3-T_4)-(T_2-T_1)}{(T_2-T_1)/[U_C A_C(\mathcal{D}_C)]+(T_3-T_4)/[U_H A_H(\mathcal{D}_H)]}, \tag{43}$$

where

$$\mathcal{D}_C=[(T_c-T_1)-(T_c-T_2)]/\ln[(T_c-T_1)/(T_c-T_2)]$$

and

$$\mathcal{D}_H=[(T_3-T_h)-(T_4-T_h)]/\ln[(T_3-T_h)/(T_4-T_h)]$$

are the log mean temperature differences [21]. It is clearly seen from Eqs. (38)–(43) that at high temperatures the coefficient of performance of a harmonic quantum Brayton refrigeration cycle consisting of two adiabatic and two constant-frequency processes is identical with that of a classical Brayton refrigeration cycle using an ideal gas as the working substance, and the cooling rate and power input are very similar to those of a classical Brayton refrigeration cycle. If $T_c/(2a\omega_1)=1/(U_C A_C)$ and $T_h/(2a\omega_2)=1/(U_H A_H)$ are chosen, Eqs. (39) and (40) are identical with Eqs. (43) and (43), respectively. This shows clearly that, in the high-temperature limit, a harmonic quantum Brayton refrigeration cycle consisting of two adiabatic and two constant-frequency processes may be equivalent to a classical Brayton refrigeration cycle using an ideal gas as the working substance [22]. Thus, such a cycle as described in the present paper may be reasonably referred to as the harmonic quantum Brayton refrigeration cycle.

VII. DISCUSSION

It is of interest to compare the results obtained here with those in Ref. [9]. It can be clearly seen that there are some

similarities and essential differences for the quantum Brayton refrigeration cycles using harmonic oscillator and spin systems as the working substance. For example, the expressions for the amounts of heat exchange Q_c and Q_h, work input W, and the coefficient of performance ε, of the quantum Brayton refrigeration cycle working with harmonic oscillators are very similar to those of the quantum Brayton refrigeration cycle working with spin-1/2 systems [9]. As another example, when the quantum Brayton refrigeration cycles working with two different working substances are operated at very low temperatures, the coefficient of performance and cooling rate decrease quickly as the temperature of the low-temperature reservoir is lowered. However, because the harmonic oscillators and spin-1/2 particles obey different statistical laws, the properties of the two kinds of systems are themselves very different under general circumstances, so that there are some essential differences for the performance characteristics of the quantum Brayton refrigeration cycles working with two different working substances. For example, the quantum Brayton refrigeration cycles working with harmonic oscillators cannot be operated across the critical temperature T_0 of BEC of the harmonic oscillator system, because an isentropic or isobaric process from the region of $T>T_0$ to that of $T<T_0$ is impossible for a Bose system [23], while the restrictive condition does not exist for quantum Brayton refrigeration cycles working with spin-1/2 particles. Even at high temperatures, the heat transfer laws are different and may be expressed, respectively, as $dQ=-[1/(\beta'\omega)]d\omega$ for harmonic oscillators and $dQ=-(\beta'\omega/4)d\omega$ for spin-1/2 particles.

In order to understand more deeply the performance of the quantum refrigeration cycle, it is significant to plot the $1/\varepsilon$-$1/R^*$ curve of an irreversible harmonic quantum Brayton refrigeration cycle at high temperatures, as shown in Fig. 8. It is seen from Fig. 8 that the characteristic curve is similar to those based on finite-time thermodynamic models [24–27] in which finite-rate heat transfer is the sole irreversibility. If the heat leak losses in the refrigeration cycle are further considered, one can generate a $1/\varepsilon$-$1/R^*$ characteristic curve which is similar to those obtained in Refs. [27], [28], in which finite-rate heat transfer and heat leak are considered simultaneously.

VIII. CONCLUSIONS

An important cycle model of the quantum refrigeration cycle using many noninteracting harmonic oscillators as the working substance and consisting of two adiabatic and two constant-frequency processes has been established. The refrigeration cycle may be reasonably referred to as the harmonic quantum Brayton refrigeration cycle. It is one of the three important quantum thermodynamic cycle models working with harmonic oscillators. On the basis of statistical mechanics, the motion equation, and the semigroup formalism, we have analyzed the general performance characteristics of the harmonic quantum Brayton refrigeration cycle and derived concrete expressions for several important parameters such as the coefficient of performance, cooling rate, power input, and rate of entropy production. By using numerical solutions, the performances of the harmonic quantum Brayton refrigeration cycle are optimized. Several optimal performance characteristic curves are generated. The optimal operating regions of some important performance parameters are determined. In general, the cooling rate is not a monotonic function of the coefficient of performance, and the optimal coefficient of performance always decreases as the cooling rate increases. However, in the high-temperature limit, the cooling rate is a monotonically decreasing function of the coefficient of performance. Consequently, consideration must be paid to both the coefficient of performance and the cooling rate. In addition, it is suggested that in the high-temperature limit the coefficient of performance of a harmonic quantum Brayton refrigeration cycle is the same as that of a classical Brayton refrigeration cycle, and the cooling rate and power input may be equivalent to those of a classical Brayton refrigeration cycle. To sum up, the results obtained here can reveal the general performance characteristics of a quantum Brayton refrigeration cycle using harmonic oscillators as the working substance and will be helpful in understanding further the relationship and distinction between quantum and classical Brayton refrigeration cycles.

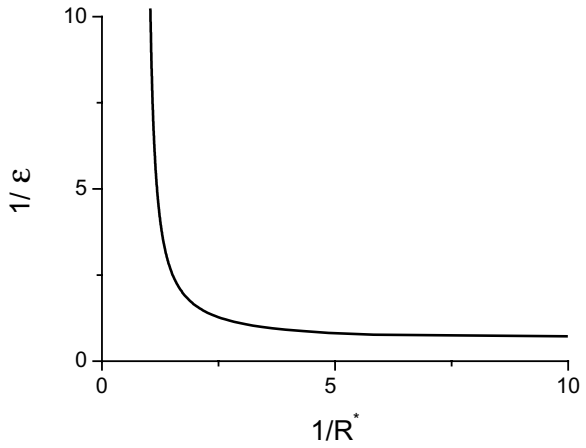

FIG. 8. The $1/\varepsilon$-$1/R^*$ characteristic curve of the cycle at high temperatures.

ACKNOWLEDGMENTS

This work has been supported by the National Natural Science Foundation, People's Republic of China and the Key Project Foundation of Science and Technology Research of the Ministry of Education, People's Republic of China.

[1] B. Lin and J. Chen, Phys. Rev. E **67**, 046105 (2003).
[2] J. Arnaud, L. Chusseau, and F. Philippe, Eur. J. Phys. **23**, 489 (2002).
[3] E. Geva and R. Kosloff, J. Chem. Phys. **97**, 4398 (1992).
[4] B. Lin, J. Chen, and B. Hua, J. Phys. D **36**, 406 (2003).
[5] R. Kosloff and M. Ratner, J. Chem. Phys. **80**, 2354 (1984).
[6] F. Wu, L. Chen, F. Sun, and C. Wu, Energy Convers. Manage. **39**, 733 (1998).

[7] J. He, J. Chen, and B. Hua, Phys. Rev. E **65**, 036145 (2002).
[8] J. Chen, B. Lin, and B. Hua, J. Phys. D **35**, 2051 (2002).
[9] T. Feldmann and R. Kosloff, Phys. Rev. E **61**, 4774 (2000).
[10] F. Wu, L. Chen, F. Sun, C. Wu, and P. Hua, Energy Convers. Manage. **39**, 1161 (1998).
[11] T. Feldmann, E. Geva, R. Kosloff, and P Salamon, Am. J. Phys. **64**, 485 (1996).
[12] E. Geva and R. Kosloff, J. Chem. Phys. **96**, 3054 (1992).
[13] P. K. Pathria, *Statistical Mechanics* (Pergamon, London, 1972).
[14] W. H. Louisell, *Quantum Statistical Properties of Radiation* (Wiley, New York, 1990).
[15] R. Alicki and K. Leudi, *Quantum Dynamical Semigroups and Applications* (Springer-Verlag, Berlin, 1987).
[16] R. Alicki, J. Phys. A **12**, L103 (1979).
[17] E. Geva and R. Kosloff, Phys. Rev. E **49**, 3903 (1994).
[18] H. Spohn and M. Ratner, J. Chem. Phys. **38**, 109 (1979).
[19] R. Kosloff, J. Chem. Phys. **80**, 1625 (1984).
[20] Z. Yan and J. Chen, J. Phys. D **23**, 136 (1990).
[21] C. Wu and R. L. Kiang, Int. J. Ambient Energ. **11**, 129 (1990).
[22] B. Lin, S. k. Tyagi, and J. Chen (unpublished).
[23] L. D. Landau and E. M. Lifshitz, *Statistical Physics* (Pergamon, London, 1958)
[24] J. Chen and Z. Yan, J. Appl. Phys. **63**, 4795 (1988).
[25] A. Bejan, Int. J. Heat Mass Transfer **32**, 1631 (1989).
[26] D. C. Agrawal and V. J. Menon, J. Phys. A **23**, 5319 (1990).
[27] J. M. Gordon and K. C. Ng, J. Appl. Phys. **75**, 2769 (1994).
[28] J. M. Gordon, K. C. Ng, and H. T. Chua, Int. J. Refrig. **20**, 191 (1997).